Semnan University

Progress in Physics of Applied Materials

journal homepage:https://ppam.semnan.ac.ir/

Synthesis ZnO/RGO nanocomposite: Structural characteristics and antifungal/antibacterial properties

Mahshid Chireh[a], Mahmoud Naseri[a,*], Maryam Rahimi[b], Ali Reza Soleymani[c]

[a]*Department of Physics, Faculty of Science, Malayer University, Malayer, Iran.*
[b]*Department of Biology, Faculty of Science, Malayer University, Malayer, Iran.*
[c]*Department of Applied Chemistry, Faculty of Science, Malayer University, Malayer, Iran.*

ARTICLE INFO

Article history:
Received: 17April 2024
Revised:12May 2024
Accepted: 19May 2024

Keywords:
Thermal treatment
Antibacterial
Antifungal
ZnO/RGO Nanocomposite

ABSTRACT

The research presented herein involves the synthesis of ZnO nanoparticles (NPs) via a simple thermal treatment approach, utilizing a solution comprising Polyvinylpyrrolidone (PVP) as capping reagent and Zn nitrate as the metal source. Subsequently, these ZnO NPs underwent a conversion process into a ZnO/RGO nanocomposite (NCs) through a simple process of polymerization. Various characterization techniques such as Fourier transform infrared spectroscopy, field emission scanning electron microscopy and X-ray diffraction, were employed to investigate the phase composition, microstructure form, and degree of crystallinity. At room temperature, Analysis using Energy dispersive X-ray analysis confirmed the presence of C, Zn, and O elements in the prepared nanocomposite composition. Surface area of the ZnO/RGO NCs was determined through the adsorption–desorption isotherms of N_2 gas using Brunauer–Emmett–Teller analysis. The antibacterial and antifungal activities of graphene, ZnO, and ZnO/RGO NCs with results from the disc agar diffusion method indicating the absence of antibacterial activity in graphene and ZnO NPs, while the ZnO/RGO nanocomposites displayed notable antifungal activity. Moreover, graphene alone did not exhibit any noticeable antifungal properties.

1. Introduction

The presence and proliferation of microorganisms (MO) on the surfaces of public places can impact the life of humans. The increasing resistance of various bacterial species to conventional antibiotics poses a significant challenge in the clinical management and bacterial infections control. While traditional bactericides have been historically effective in controlling bacteria, concerns over their environmental and human health impacts have restricted their continued use. The rise in bacterial resistance has further limited the applicability of these materials. To overcome these challenges, the application of antimicrobial agents has concerned as a promising solution [1]. Nanotechnology has significantly influenced various scientific fields such as nanomedicine, biomedicine, biosensors, smart city development, energy, and environmental sectors. Nanoparticles (NPs), known for their antimicrobial properties, have demonstrated efficacy against pathogens, gram-negative and gram-positive bacteria, and other microorganisms over the years. Metal oxide NPs, with their large surface area, act as potent antimicrobial agents [2]. Metals and their oxides NPs, including AgO, ZnO, CoO, and CuO NPs, have shown promise in bacterial growth inhibition, and wound healing promotion, as well as medical imaging, targeted drug delivery, and cancer therapy, garnering considerable attention from researchers. Unlike organic NPs, metal NPs offer advantages in antimicrobial/ fungicidal properties due to their considerable stability, durability, and robustness, and also minimal toxicity to mammalian cells. Their nanoscale size and versatile surface chemistry enable them to cause bacterial toxicity via mechanisms such as, oxidative stress, lipid peroxidation,

* Corresponding author.
E-mail address: mahmoud.naseri55@gmail.com

Cite this article as:
Chireh, M., naseria, M., Rahimi, M. and Soleymani AR., 2024.Synthesis ZnO/RGO nanocomposite: Structural characteristics and antifungal/antibacterial properties. *Progress in Physics of Applied Materials*, 4(1), pp.77-81.DOI: 10.22075/PPAM.2024.33663.1094

cell membrane disruption and enzyme inhibition [3]. Reduced graphene oxide (RGO) finds applications in the biomedical fields and can be utilized to modify physicochemical properties of metal oxide NPs like Zinc Oxide [4]. Graphene oxide, along with graphene/metal oxide composites, has gained significant interest due to its cost-effectiveness, accessibility, and compatibility with diverse substrates [4, 5]. In the current research endeavor, zinc oxide NPs were synthesized using an aqueouszinc nitrate and polyvinyl pyrrolidone, through a thermal treatment method completed by grinding and calcination. This synthesis approach, which excludes the addition of other chemicals, offers advantages in terms of simplicity, cost-effectiveness, low reaction temperature, minimal by-product generation, and eco-friendliness [6]. In addition, using the ZnO NPs, along with Reduced Graphene Oxide (RGO) nanosheets, the ZnO/RGO NCs was prepared. Structural characteristics of the samples were determined in details and the antifungal/antibacterial properties of the samples were evaluated.

2. Materials and methods

2.1. Preparation of ZnO NPs

To synthesize ZnO NPs, a simple thermal treatment method was employed. Initially, 4 g of PVP (as a capping agent to stabilize the nanoparticles and prevent them from agglomeration) were dissolved in 100 ml of hot deionized water (80˚C). Subsequently, 0.0297 g of $Zn(NO_3)_2.6H_2O$ were inserted to the polymer solution and mixed for 2 hours severely. The solution underwent heating in an oven at 100˚C for 24 hours to complete evaporation of water. The resulting dried precursor was then crushed and ground in a mortar to obtain powder form. The powder underwent calcination at 550˚C for 3 hours to oxidize the Zinc oxide as well as eliminate any organic residues, and facilitate the crystallization of the formed ZnO nanoparticles.

2.2. Preparation of ZnO /RGO NCs

A simple polymerization method was employed to convert the ZnO NPs into ZnO/RGO NCs. The previously synthesized Graphene Oxide (GO), obtained from graphite powder using a modified Hummers method (as described in prior research [7]), was dispersed in deionized water and sonicated subsequently, the prepared ZnO nanoparticles were added to the suspension and stirred to achieve a uniform dispersion. Hydrazine hydrate was then introduced to the mixture and stirred for 60 minutes. The suspension underwent centrifugation and washing with ethanol and deionized water.The resulting product, aimed at obtaining the ZnO/RGO nanocomposite, was dried at 60 ˚C under vacuum condition for 24 hours.

2.3. Characterization

The crystalline phase of the synthesized ZnO NPs and ZnO/RGO NCs was ascertained at ambient temperature using an X-Ray Diffractometer (XRD) with CuKα radiation (λ= 0.15406 nm) on an X'Pert PRO MPD instrument. Fourier Transform Infrared (FT-IR) spectra were recorded on a PerkinElmer FTIR 1650 spectrometer to assess the chemical bonds in the NCs. The microstructure of the samples was analyzed using a JEOL JSM-6701 F-type instrument coupled with Energy Dispersive X-ray Spectroscopy (EDX) for elemental analysis. The surface area of the samples was determined using the Brunauer–Emmett–Teller (BET) method with a Micrometrics Belsorp mini system, while the pore-size distribution was assessed by nitrogen adsorption at 77 K.

2.4. Antibacterial and Antifungal activity evaluation

The antimicrobial ability of graphene, ZnO and ZnO/RGO NCs was tested by means of the disc agar diffusion method. In this regard, two locally isolated and identified bacterial test strains, Escherichia coli IRAQ3 (Gram-negative bacterium, acc. no. MH 782077) and Staphylococcus aureusS33R (Gram-positive bacterium, acc. no.NR–o37007.2) were utilized. The standard fungus strain, Candida albicans (C. albicans) with the reference number PTTC10231, was sourced from the Iranian Center of Industrial Bacteria and Fungi Collection in Tehran, Iran. For each test strain, 100µl of cell suspension (107–108 cfu/mL) were aseptically swabbed over the surface of nutrient agar plates. Subsequently, 2 grams of each sample, were located on the surface of the inoculated plates and then refrigerated at 4 °C for 2 hours to allow nutrient medium to be saturated with the pathogenic strains. Following this, the plates were transferred to an incubator set at 37°C for 24 hours, and the bacterial inhibitions were identified based on the formation of clear zones (mm) around the samples [7, 8].

3. Results and discussion

3.1. Structural and morphological characteristics

The crystal structure and phase purity of ZnO NPs and ZnO/RGO NCs were explored by XRD analysis. Figure1 illustrates the prominent peaks in the XRD pattern of samples. The distinct peaks observed at 2θvalues of 32.26°, 34.86°, 36.48°, 47.85°, 56.88°, 63.40°, 66.44°, 68.39°, 69.12°, and 76.98° in the XRD patterns of ZnO nanoparticles correspond to the crystal planes (100), (002), (101), (102), (110), (103), (200), (112), (201), and (202), respectively. These peaks confirm the presence of ZnO in the hexagonal wurtzite phase (ICDD PDF: 79-0205) [4]. It should be noted that the XRD results obtained in this study align with the findings from previous research on ZnO/SiO_2 NCs [4], with minor shifts observed in the 2θ values.

The XRD pattern of the ZnO/RGO NCs also exhibits picks correlating with the hexagonal wurtzite phase of ZnO NPs. Additionally, a peak in the 2θ range of 20-30° was indicates the presence of graphene nanosheet within the nanocomposite. The appearance of RGO peaks validates the successful synthesis of ZnO/RGO NCs. The average crystal sizes of 48 and 65 nm were calculated for ZnO NPs and ZnO/RGO NCs, respectively, using the Debye-Scherrer formula as described by Equation 1 [9]:

$$D=0.9\lambda/\beta\cos\theta \quad (1)$$

Where D represents the crystallite size, λ is the X-ray radiation wavelength, β is the full width at half maximum (FWHM) of the peak, and θ is the Bragg angle.

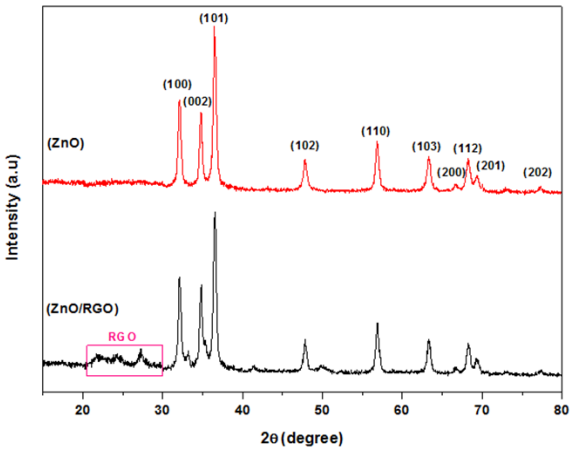

Fig. 1.XRD patterns of ZnO NPs and ZnO/RGO NCs.

Fig. 2 represents the FESEM image and EDX analysis for ZnO/RGO NCs. In Fig. 2a, the FESEM image illustrates quasi-spherical nanostructures of ZnO NPs in the ZnO/RGO NCs. It is evident from the image that some ZnO nanoparticles exhibit aggregation, with particles deposited both on and between the RGO sheets. The ZnO average particle size in the NCs was determined to be approximately 38 nm.

Fig. 2b displays the results of the EDX analysis carried out to assess the NCs chemical composition. The EDX spectrum reveals the presence of Zn, O, and C elements in the ZnO/RGO NCs.

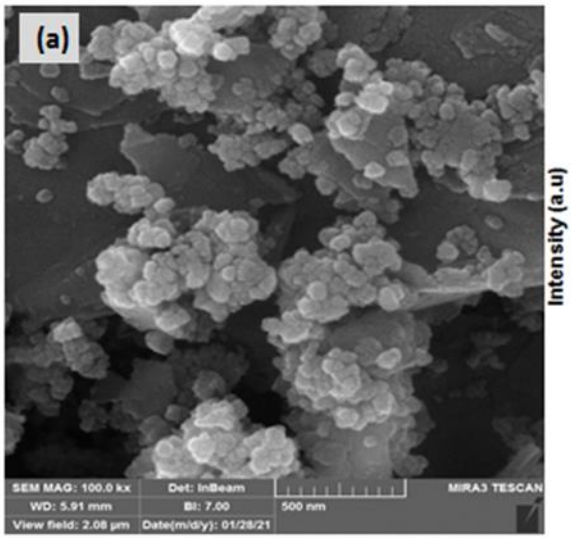

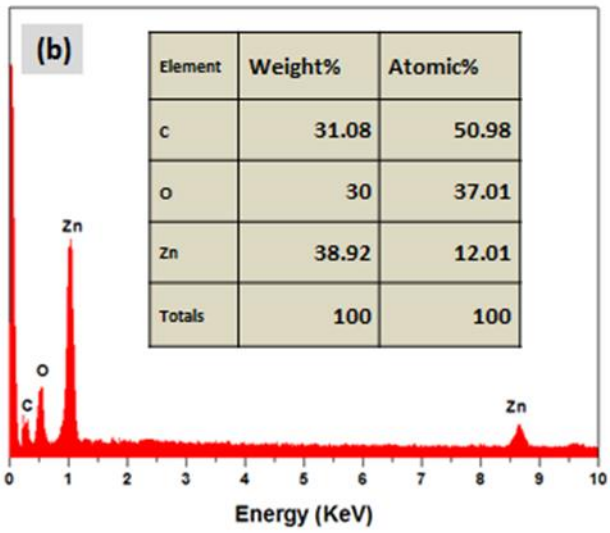

Fig. 2.(a) FESEM images and (b) EDX analysis of ZnO/(RGO NCs)

Fig. 3 illustrates the FTIR spectra of the prepared ZnO/RGO NCs. The main absorption band corresponding to Zn–O bond is observed at 469 cm^{-1}, confirming the existence of zinc oxide in the NCs [10, 11]. The peak at 1109 cm^{-1} is attributed to the alkoxy C-O stretching vibration [7]. Additionally, the absorption bands at 1588 cm^{-1} correspond to the asymmetric and symmetric stretching vibrations of C=O bonds related to the Zn–OH mode, respectively [11]. The peaks at 2925 and 2827 cm^{-1} are associated with the asymmetric and symmetric vibrations of C–H bonds [12]. The small peaks in the range of approximately 1200- 1500 cm^{-1} are assigned to the carboxyl and carbonyl groups in the NCs [13]. Furthermore, the broad peak at 3402 cm^{-1}in the FTIR spectrum is likely referred to the O–H stretching vibration of H_2O presented and the C–OH groups [14, 15].

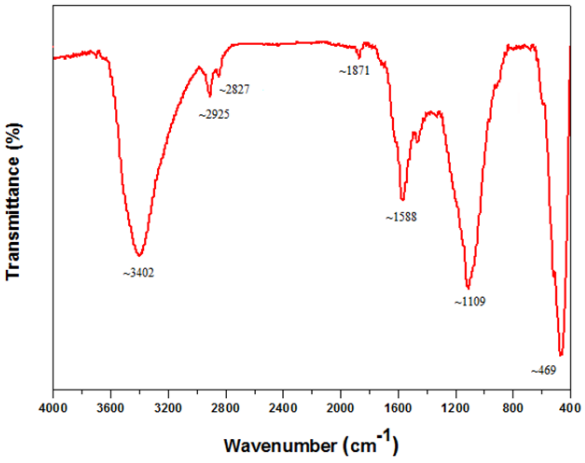

Fig. 3. FTIR spectra of ZnO/RGO NCs.

3.2. BET surface analysis

The surface properties of the samples were assessed using the BET analysis at 77 K. Figures 4(a) and 4(b) present the BET surface area of, and the corresponding BJH pore size distribution in the ZnO/RGO NCs. Figure 4(a) reveals type IV adsorption isotherms with hysteresis loops, indicating the presence of mesopores in the ZnO/RGO NCs.

The observed distinct hysteresis loop is attributed to the existence of mesopores within the NCs structure. The pore average diameter in the ZnO/RGO NCs was estimated to be 29.35 nm, with a specific surface area of 15.77 m^2g^{-1}. The large specific surface area and even thedistribution of NPs within the ZnO/RGO NCs suggest the presence of abundant adsorption and reaction sites. This reveals that the formation of pores can enhance the surface area activity, potentially leading to improved adsorption capabilities and reactivity within the NCs [16].

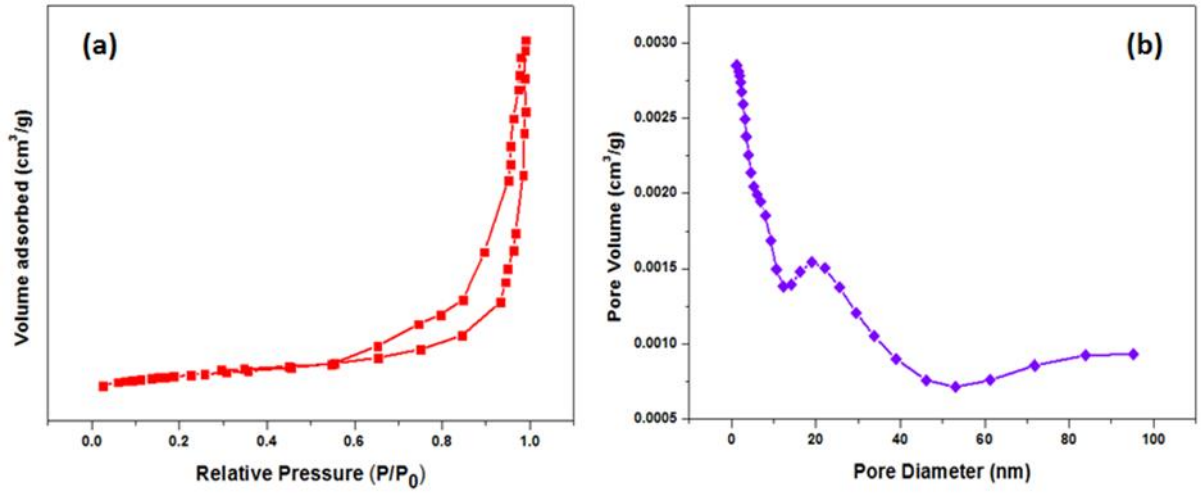

Fig.4. (a) Nitrogen adsorption–desorption isotherms, and (b) corresponding pore size distribution of ZnO/RGO P.

3.3. Antibacterial and Antifungal activity assessment

The antibacterial activity of the prepared ZnO/RGO NCs, along with RGO, did not exhibit any observable inhibition zones. However, the antifungal activity of ZnO/RGO NCs showed inhibition zones. Specifically, the ZnO and ZnO/RGO nanocomposites displayed inhibition zone values of 35 mm and 37 mm against C. albicans, respectively. In contrast, the antifungal activity of RGO alone was not observed. These findings are in agreement with previous studies demonstrating the remarkable antifungal properties of Zn-based composites, which have been shown to induce deformation in fungal hyphae. [17, 18]. Hence, the enhanced antifungal activity of the synthesized ZnO/RGO NCs, underscoring the potential of these materials for applications in antimicrobial treatments. Future research could further explore the mechanisms underlying the antifungal properties of the ZnO/RGO NCs and their potential for practical implementation in various fields.

4. Conclusion

In this research, ZnO NPs were successfully synthesized using a simple thermal treatment method, and utilized for the preparation of ZnO/RGO NCs through a subsequent polymerization process. The outstanding outcomes of the work can be stated as follows:

- The XRD pattern confirmed the presence of a hexagonal wurtzite structure for the ZnO NPs.
- The FESEM imaging revealeddeposition of ZnO NPs on the grapheme nanosheets.
- Both ZnO NPs and ZnO/RGO NCs demonstrated notable antifungal activity, whereas RGO did not exhibit any antifungal properties.
- No one of the prepared samples showed antibacterial activity.

Acknowledgements

There is nothing to acknowledgement.

Conflicts of Interest

The author declares that there is no conflict of interest regarding the publication of this article.

References

[1] Shih, K. Y., and Yu, S. C., 2021. Microwave-Assisted Rapid Synthesis of Eu $(OH)_3$/RGO Nanocomposites and Enhancement of Their Antibacterial Activity against Escherichia coli. Materials, 15(1), 1-17.

[2] Choudhary, A. K., Gupta, A., Kumar, S., Kumar, P., Singh, R. P., Singh, P., and Kumar, V., 2020. Synthesis, Antimicrobial Activity, and Photocatalytic Performance of Ce Doped SnO_2 Nanoparticles. Frontiers in Nanotechnology, 11.

[3] Haghniaz, R., Rabbani, A., Vajhadin, F., Khan, T., Kousar, R., Khan, A. R., and Wahid, F., 2021. Anti-bacterial and wound healing-promoting effects of zinc ferrite nanoparticles. Journal of Nanobiotechnology, 19(1), 1-15.

[4] Chireh, M., Karam, Z. M., Naseri, M., Jafarinejad-Farsangi, S., and Ghaedamini, H., 2022. Synthesis, characterization and cytotoxicity study of graphene/doped ZnO/SiO_2 nanocomposites. Applied Physics A, 128(4), 1-8.

[5] Alamdari, S., SasaniGhamsari, M., Afarideh, H., Mohammadi, A., Geranmayeh, S., JafarTafreshi, M., Ehsani, M. H., Majles ara, M. H., 2019. Preparation and characterization of GO-ZnO nanocomposite for UV detection application. Optical Materials, 92 243-250.

[6] Ghasemi, R. Naseri, M. Souri, D. Kamalianfar, A., 2022. Structural and physical properties of $Co_{1-x}Cd_xFe_2O_4$ /SiO_2 nanocomposites, PPAM. 2 147-156.
[7] Chireh, M., Naseri, M., and Ghiasvand, S., 2019. Enhanced photocatalytic and antibacterial activities of RGO/$LiFe_5O_8$ nanocomposites. Journal of Photochemistry and Photobiology A: Chemistry, 385, 112063.
[8] Youssef, A. M., Abdel-Aziz, M. S., and El-Sayed, S. M., 2014. Chitosan nanocomposite films based on Ag-NP and Au-NP biosynthesis by Bacillus subtilis as packaging materials. International journal of biological macromolecules, 69, 185-191.
[9] Chireh, M., Naseri, M., and Kamalianfar, A., 2020. 57Fe Mossbauer spectroscopy investigation of $NiFe_2O_4$ and $MnFe_2O_4$ ferrite nanoparticles prepared by thermal treatment method. Applied Physics A, 126(7), 1-6.
[10] Chireh, M., and Naseri, M., 2019. Effect of calcination temperature on the physical properties of $LiFe_5O_8$ nanostructures. Advanced Powder Technology, 30(5), 952-960.
[11] Mohamed, M. B., Abdel-Kader, M. H., and Alhazime, A. A., 2019. Structural and optical properties of doped ZnO/SiO_2 nanocomposite. International Journal of Applied Ceramic Technology, 16(3), 1209-1217.
[12] Durmus, Z., Kurt, B. Z., and Durmus, A., 2019. Synthesis and characterization of graphene oxide/zinc oxide (GO/ZnO) nanocomposite and its utilization for photocatalytic degradation of basic fuchsin dye. ChemistrySelect, 4(1), 271-278.
[13] Alamdari, S., Ghamsari, M. S., Afarideh, H., Mohammadi, A., Geranmayeh, S., Tafreshi, M. J., and Ehsani, M. H., 2019. Preparation and characterization of GO-ZnO nanocomposite for UV detection application. Optical Materials, 92, 243-250.
[14] Sheshmani, S., and Nayebi, M., 2019. Modification of TiO_2 with graphene oxide and reduced graphene oxide; enhancing photocatalytic activity of TiO_2 for removal of remazol Black B. Polymer Composites, 40(1), 210-216.
[15] Mudila, H., Rana, S., and Zaidi, M. G. H., 2016. Electrochemical performance of zirconia/graphene oxide nanocomposites cathode designed for high power density supercapacitor. Journal of Analytical Science and Technology, 7(1), 1-11.
[16] Lin, Y., Dong, J., Dai, J., Wang, J., Yang, H., and Zong, H., 2017. Facile synthesis of flowerlike $LiFe_5O_8$ microspheres for electrochemical supercapacitors. Inorganic chemistry, 56(24), 14960-14967.
[17]Lili, H.,Yang, L.,Azlin ,M., Mengshi, L., 2011. Antifungal activity of zinc oxide nanoparticles against Botrytis cinerea and Penicillium expansum. Microbiological Research, 166(3), 207-215.
[18] Hashemi, A., Tavafi, H., Naseri, M., Mojtabazadeh, H., abedi, M., tork, N., 2024. Structural and antibacterial properties of $AgFe_2O_4$, Fe_3O_4 nanoparticles and their nanocomposites. PPAM 4 (2024) 37-46.